Dyes and Pigments 92 (2012) 1160–1165

Contents lists available at ScienceDirect

Dyes and Pigments

journal homepage: www.elsevier.com/locate/dyepig

A near-infrared dye for dye-sensitized solar cell: Catecholate-functionalized zinc phthalocyanine

Ashis K. Sarker [a], Man Gu Kang [b], Jong-Dal Hong [a,*]

[a] Department of Chemistry, University of Incheon, 12-1 Songdo-dong, Yeonsu-gu, Incheon 406-772, Republic of Korea
[b] Convergence Components and Materials Research Laboratory, Electronics and Telecommunication Research Institute (ETRI), Daejeon 305-350, Republic of Korea

ARTICLE INFO

Article history:
Received 22 April 2011
Received in revised form
3 July 2011
Accepted 5 July 2011
Available online 19 July 2011

Keywords:
Catechol-functionalized zinc phthalocyanine
NIR dyes
Dye-sensitized solar cell
Anchoring groups
Photovoltaic windows

ABSTRACT

The design and synthesis of an asymmetrical zinc phthalocyanine sensitizer modified with a catechol anchoring group is reported. The performance of this sensitizer was evaluated in a dye-sensitized solar cell. A strong interaction between the catechol dye and TiO_2 (with the formation of a five-membered charge-transfer complex) was evidenced by a strong shift in the Q-band of the *ZnPc-Cat* from 680 nm in solution to 750 nm on TiO_2, along with an appreciable absorption tail extending to ~1000 nm. The fabricated solar cell containing the phthalocyanine sensitizer showed relatively high light-to-electron conversion efficiency (η = 0.92%), considering that few catechol dyes exceed η = 0.7% in dye-sensitized solar cells. Values of I_{sc} = 2.53 mA cm^{-2} and V_{oc} = 540 mV were obtained, referring to a standard N719 cell (η = 6.46%). A comparison of zinc phthalocyanine sensitizers bearing different anchoring groups affirmed the superiority of carboxylate groups relative to those bearing catechol groups in terms of cell performance.

1. Introduction

The development of alternative energies have become an important issue due to the global impact and rapidly growing threats to the natural and living environment resulting from population growth, increased energy demands, climate changes, and natural resource depletion. Among the alternative energy sources identified to date, solar energy has been widely recognized as a major sustainable and clean energy supply because of the abundance and safety of the source. Dye-sensitized solar cells (DSSCs) have attracted considerable attention as a possible candidate for low-cost photovoltaic cells. The heart of this cell is a photoanode, consisting of a nanoporous TiO_2 film covered by a monolayer of photosensitizer [1–3]. For the design of highly efficient sensitizers, at least three conditions must be met; a large spectral overlap with the solar emission spectrum, fast electron injection into the conduction band of the semiconductor, and slow charge recombination between the injected electron and the sibling dye cation. The most successful sensitizers employed in these cells to date are polypyridylruthenium complexes, which yield solar energy-to-electric power conversion efficiencies of 10–11% with simulated sunlight [4]. However, the main drawback of ruthenium-based sensitizers is their lack of absorption in the red region of the visible spectrum. In addition, the anchoring groups of the major dyes reported so far are carboxylates, which show some disadvantages; typically, slow desorption of the sensitizers. The desorption of the photosensitizers has been attributed to the weak binding to TiO_2 resulting from the low pK_a values of the carboxylates (pK_a ~3.5) [5–7], which limits the long-term DSSC stability. Phosphonate anchoring groups (pK_a ~6.5) [8–10] are known to give improved dye binding stability on TiO_2 compared with carboxylate groups [11]. Catecholate (pK_a ~9.6) has been reported to bind to TiO_2 more strongly than any other types of anchoring group, due to the formation of a five-membered charge-transfer (CT) complex with TiO_2 nanoparticles [12,13].

Enediol units of catechol tend to bind strongly to TiO_2 through the chelation of surface Ti(IV) ions, giving rise to intense dye-to-TiO_2 charge-transfer (DTCT) bands [12,14–20], that appear at wavelengths longer than 320 nm, along with local bands arising from the dye itself. Several reports have demonstrated that the photoexcitation of DTCT bands give rise to very fast (<100 fs) direct electron injection from the dyes to TiO_2 [21–24], in compliance with Mulliken's CT theory [25]. These types of dyes contrast with those, that, upon light absorption, are first excited from the highest occupied molecular orbital (HOMO) to the lowest unoccupied molecular orbital (LUMO), and inject electrons from the excited state into the TiO_2 conduction band.

* Corresponding author. Tel.: +82 32 835 8234; fax: +82 32 835 8238.
E-mail address: hong5506@incheon.ac.kr (J.-D. Hong).

0143-7208/$ – see front matter © 2011 Elsevier Ltd. All rights reserved.
doi:10.1016/j.dyepig.2011.07.002

Here we examined phthalocyanines (Pc), which are an excellent alternative material for solar cell applications, due to their intense absorption in the red/near-IR regions [12,13,26]. We designed an asymmetrical zinc phthalocyanine, functionalized with a catechol anchoring group (*ZnPc-Cat*, chemical structure in Scheme 1) containing three tert-butyl groups. The energy band structure of *ZnPc-Cat* was determined using cyclic voltammetry (CV). The effects of catecholate and carboxylic acid anchoring groups on photovoltaic cells sensitized with two types of zinc phthalocyanine with exactly equivalent chemical structures were explored using the strategy outlined in Scheme 1.

2. Results and discussion

2.1. Synthesis of ZnPc-Cat

The synthesis of *ZnPc-Cat* was carried out using the reaction route outlined in Scheme 1. First, 4,5-dicyano-2,2-dimethyl-1,3-benzodioxole (**3**) was obtained from pyrocatechol using the following sequential reaction steps: Benzodioxole protection of the hydroxyl groups, bromination of the benzene ring, and cyanation of the resulting dibromide (**2**) (following an earlier report) [27]. The *ZnPc*-benzodioxole (**4**) was prepared by the cyclization reaction of (**3**) and 4-tert-butyl-phthalonitrile with $Zn(OAc)_2 \cdot H_2O$ in pentanol, using DBU (1,8-diazabicyclo[5.4.0]undec-7-ene) as the base [8]. This was followed by column chromatographic purification on silica gel. The final product *ZnPc-Cat* (**5**) was obtained as a dark blue powder by elimination of the benzodioxole protection group from **4**. *ZnPc-Cat* was characterized using ^{1}H NMR, IR spectroscopy, and MALDI-TOF-MS. The mass spectrum of *ZnPc-Cat* (Fig. 1) was consistent with the designed structures. The *ZnPc-Cat* exhibited moderate solubility in common organic solvents such as chloroform, chlorobenzene, and dichlorobenzene.

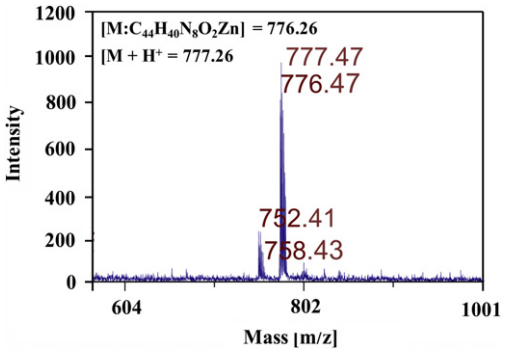

Fig. 1. Mass spectrum of *ZnPc-Cat*.

2.2. UV/visible absorption and fluorescence spectra

The absorption spectrum of *ZnPc-Cat* in a diluted ethanol solution (3% v/v) was compared with *ZnPc-Cat* bound on TiO_2, as shown in Fig. 2. The absorption maximum (Q-band) of *ZnPc-Cat* was strongly shifted from 680 nm in solution to 750 nm on TiO_2. This was accompanied by a broadening of the visible band up to 800 nm and an appreciable absorption tail extending to ~1000 nm. These changes were ascribed to the DTCT bands, caused by the strong interaction between the catechol dye and TiO_2. The emission spectrum of *ZnPc-Cat* in 3% ethanol solution ($\lambda_{ex} = 350$ nm) showed a broad band in the 650 nm–710 nm region, with an emission maximum at 680 nm (Fig. 3(B)). Upon the addition of an aqueous dispersion of TiO_2 nanoparticles to the aqueous sensitizer solution, the luminescence was found to be completely quenched. The complete quenching of the emission band was ascribed mainly to direct electron injection from *ZnPc-Cat* to the TiO_2 nanoparticles. These results confirmed that electron transfer from the metal centers to the semiconductor through the catecholate moiety of *ZnPc* complex was occurring.

2.3. Electrochemical studies

ZnPc-Cat was found to be soluble in tetrahydrofuran (THF) to a maximum concentration of ~0.5 mM–1.0 mM. CV was carried out at an ITO glass electrode in a three electrode cell, using 0.1 M tetrabutylammonium perchlorate (TBAP) in anhydrous THF as the supporting electrolyte. The *CV* curve for *ZnPc-Cat* was recorded relative to a SCE reference electrode, as shown in Fig. 3. Note that the SCE was calibrated using a ferrocene–ferrocenium (Fc/Fc^+) redox couple (4.8 eV below the vacuum level) as an external standard [28].

Electrochemical analysis of *ZnPc-Cat* using cyclic voltammetry showed an onset oxidation potential of 0.58 V and an onset reduction potential of −0.95 V. The HOMO and LUMO energy level of *ZnPc-Cat* were estimated to be 4.98 and 3.45 eV respectively, from the onset oxidation and reduction potentials, using ferrocene as reference ($E_{HOMO} = 4.8$ eV) [28]. The band gap of *ZnPc-Cat* was calculated to 1.5 eV.

2.4. Photovoltaic studies

The performance of *ZnPc-Cat* was evaluated in a typical DSSC with screen-printed and double-layer films composed of an 8 μm

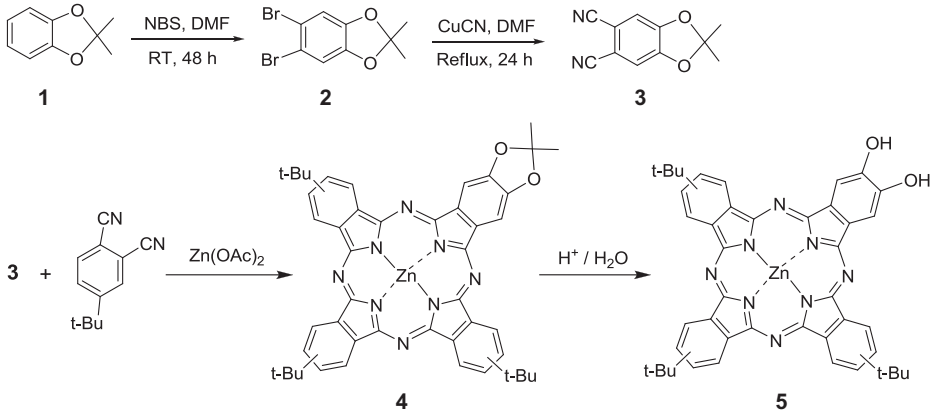

Scheme 1. The synthetic route to zinc phthalocyanine with catecholate functionality.

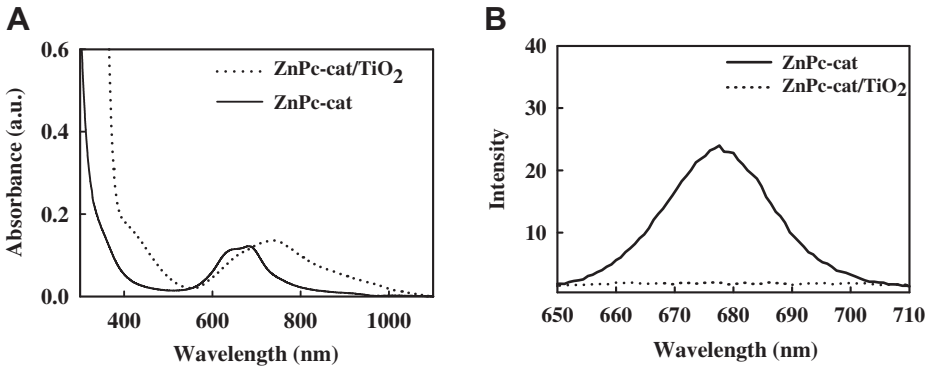

Fig. 2. (A) Optical absorption spectra of *ZnPc-Cat* in 3% ethanol solution and on TiO_2 nanoparticle surface. (B) Emission spectra of *ZnPc-Cat* in 3% ethanol solution (solid line) and on TiO_2 nanoparticles (dotted line).

transparent layer and a 4 μm scattering layer, which was treated with a 0.05 M titanium tetrachloride solution using a previously described procedure [4]. Photovoltaic measurements were carried out on the electrodes, which were dipped in ethanol/dye solutions containing chenodeoxycholic acid (to minimize the aggregation of the phthalocyanine).

Fig. 4(A) shows the photocurrent action spectrum obtained from a sandwich cell using an electrolyte containing 0.6 M 1-butyl-3-methylimidazolium iodide, 0.05 M iodine, 0.05 M LiI, and 0.5 M tert-butylpyridine in a 50:50 (v/v) mixture of valeronitrile and acetonitrile. The incident monochromatic photon-to-current conversion efficiency (IPCE, plotted as a function of excitation wavelength) reached 20%, which is relatively high for DSSCs using a sensitizer with catecholate functionality. The photocurrent action spectra were consistent with the UV–visible absorption spectra. The current–voltage characteristics of the *ZnPc-Cat*-sensitized cell (Fig. 4(B)) gave a short-circuit photocurrent density (I_{sc}) of 2.53 mA cm^{-2}, an open-circuit voltage (V_{oc}) of 540 mV, and a fill factor of 0.92, corresponding to an overall conversion efficiency (η) of 0.92% under standard global air mass (AM 1.5) solar conditions.

In the development of highly efficient DSSC dyes, carboxylic acid anchoring groups have been revealed to possess a unique advantage in terms of cell performance over other groups such as phosphonates, sulfonic acids, catechols, and nitriles [8–11]. The reasons for the improved cell performance of carboxylic acid groups are not yet clear. However, even with the use of carboxylic acid groups, the binding stability must still be improved through the use of other anchoring groups, with higher pK_a values. Thus, it is worth making a direct comparison between asymmetrical zinc phthalocyanines functionalized with either catecholate (*ZnPc-Cat*, Scheme 2) or carboxylic acid (TT1, Scheme 2), which have exactly equivalent chemical structures except the anchoring groups. The photovoltaic parameters of the two dyes are compared in Table 1. Note that the TT1 data were adopted from an earlier report by Reddy et al. [26]. In this case, the TT1-sensitized cell showed better cell performance. This is illustrated by much higher I_{sc} value compared with the *ZnPc-Cat*-sensitized cell (6.50 versus 2.53 mA cm^{-2}). This indicates the superiority of carboxylic acid groups over catechols as anchoring groups, even though the direct comparison of their photovoltaic characteristics cannot be justified, due to their absolute dependency on the skill applied in the manufacture of the cell. The photovoltaic data for a standard sensitizer N719 (Table 1) indicate the level of cell manufacturing skill. It is worth noting that the photovoltaic data for TT1 were provided by Grätzel's Lab, which reported a record cell efficiency of about 11% with an N719-sensitized DSSC [4].

The poor performance of the *ZnPc-Cat*-sensitized solar cell could be ascribed to the strong and fast recombination reaction between the injected electrons and the parent cations, which has been observed in a series of newly designed catecholate-based sensitizers, including ruthenium(II)-polypyridyl complexes [29,30], porphyrin-catechols [31], the osmium(II) polypyridyl complexes [32]. Especially, in the case of the porphyrin-catechol sensitizers, the majority of the injected electrons recombined with the parent

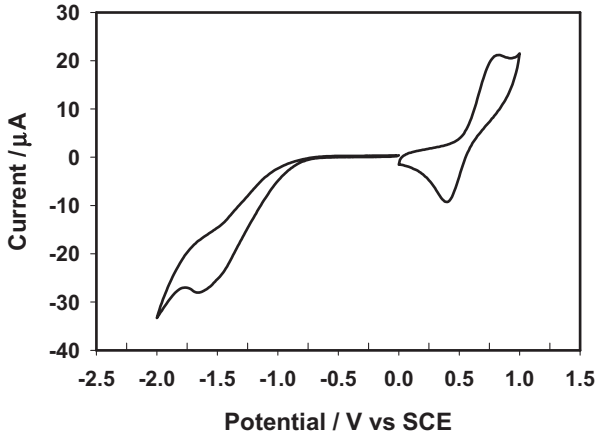

Fig. 3. Cyclic voltammograms of 0.5 mM *ZnPc-Cat*. Dry tetrahydrofuran containing 0.1 M tetrabutylammonium perchlorate was used as supporting electrolyte. Scans are initiated at 0 V versus SCE in positive and negative direction at the rate of 50 mV/s. The solutions were purged with nitrogen and stirred for over 15 min prior to the measurements.

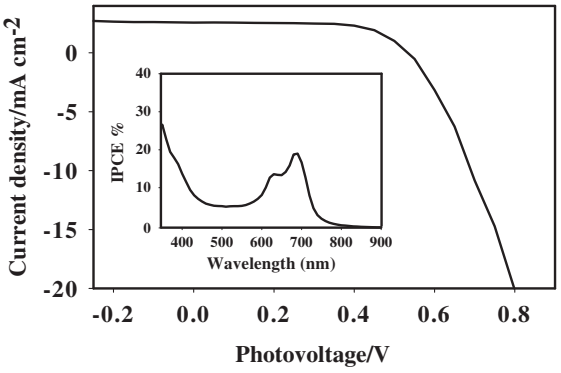

Fig. 4. Photocurrent–photovoltage characteristics of sandwich solar cells based on the *ZnPc-Cat* electrode, and photocurrent action spectra of sandwich solar cells based on a (*ZnPc-Cat*-TiO_2) film electrode using iodide/triiodide electrolyte (Inset).

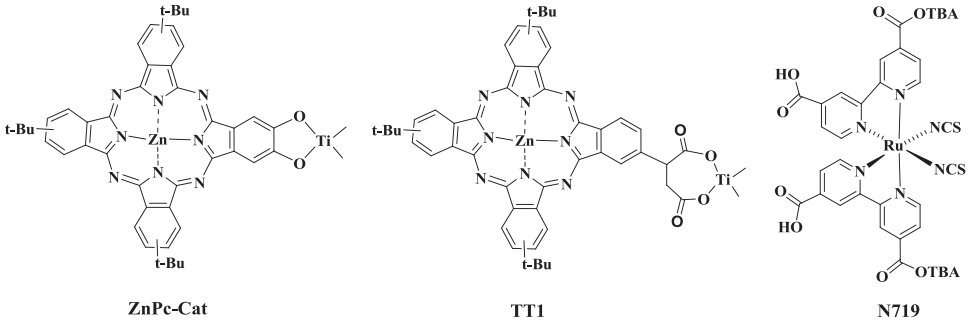

Scheme 2. The chemical structures of *ZnPc-Cat*, TT1 and N719.

Table 1
The photovoltaic parameters of the *ZnPc-Cat*, TT1 and N719 dye.

Dyes	V_{oc} [mV]	J_{sc} [mA cm^{-2}]	η [%]	*FF*
ZnPc-Cat	540	2.53	0.92	0.68
TT1[a]	635	6.50	3.05	0.74
N719	760	12.05	6.46	0.68

[a] The photovoltaic data was extracted directly from the paper of Reddy et al. [26].

cation radicals with a time constant of ~800 fs, due to the strong coupling in the dye–nanoparticle system [31].

3. Conclusions and perspectives

Red/NIR dyes are a key element in the development of dye-sensitized solar cells that can be employed as photovoltaic windows, which would transmit part of the visible light and harvest in the red/NIR part of the solar spectrum. In this article, we described the synthesis of a zinc phthalocyanine modified with a catecholate anchoring group for application in DSSCs, which improved the long-term cell efficiency. In the UV/Vis absorption spectrum of *ZnPc-Cat*/TiO_2, a DTCT band caused by the strong interaction between the catechol dye and TiO_2 was evidenced by a strong shift of *ZnPc-Cat*'s Q-band from 680 nm to 750 nm, along with an appreciable tail extending to 1000 nm. The *ZnPc-Cat*-sensitized solar cell showed a relatively high light-to-electron conversion efficiency ($\eta = 0.92\%$), considering that few catechol dyes exceed $\eta = 0.7\%$ in DSSCs. Values of $I_{sc} = 2.53$ mA cm^{-2} and $V_{oc} = 540$ mV were obtained, referring to a standard N719 cell ($\eta = 6.46\%$).

A comparison of *ZnPc* sensitizers with different anchoring groups indicated that carboxylate groups were more superior to catechol, in terms of cell performance. The poor cell performance of *ZnPc-Cat* versus *ZnPc*-carboxylate could be ascribed to the strong and fast recombination reaction between the injected electrons and the dye cations, which has been observed frequently for catechol-type dyes [33]. The strong interaction between catechol and TiO_2 contributed to an improvement in the stability of the DSSC, but simultaneously enhanced the back electron transfer rate, which lowered the cell performance. The findings should assist the design of new, highly efficient sensitizers for DSSCs.

4. Experimental section

4.1. Materials

Copper cyanide, Zinc acetate dihydrate, N,N-dimethylamino ethanol, Titanium chloride (99.9%), titanium(IV) isopropoxide (97%), acetonitrile, 1,8-diazobicyclo[5,4,0]undec-7-ene (98%), valeronitrile, iodine, 4-tert-butylpyridine, guanidinium thiocyanate were purchased from Sigma–Aldrich and used as received. 4-tert-butylpyridine, 2,2-dimethyl-1,3-benzodioxole, chenodeoxycholic acid, 4-tert-butyl-phthalonitrile were obtained from TCI. *N*-bromosuccinimide NBS (Aros organics) was purified by the recrystallization in water and dimethylformamide DMF (Samchun chemicals 99%) was distilled over molecular sieves. F-doped tin-oxide (FTO glass, 8 Ω cm^{-1}, $d = 100$ μm) and thermoplastic film (Surlyn, $d = 100$ μm) were purchased from Libby Owens Ford, and DuPont, respectively.

1-Hexyl-2,3-dimethylimidazolium Iodide >98% (C-TRI), 1-Butyl-3-methylimidazolium Iodide 98% (C-TRI), TiO_2 paste 20 (Solaronix), Ti-Nanoxide 300 (SOLARONIX), Pt-Catalyst T/SP (SOLARONIX), Trifluoroacetic acid (Fluka 99.5%), were purchased and used as received.

4.2. Preparation of 5,6-dibromo-2,2-dimethyl-1,3-benzodioxole (**2**)

N-Bromosuccinimide (50.31 g, 280 mmol) was added to 2,2-dimethyl-1,3-benzodioxole (**1**) (20 mL, 140 mmol), which was dissolved in DMF (250 mL) at room temperature. The mixture was stirred in darkness for two days. After the completion of the reaction, triple volume of water was added to the mixture. The mixture had been kept in a refrigerator overnight, whereby a white precipitate was observed. The precipitate as pure product was filtered and dried in high vacuum. The yield of 5,6-dibromo-2,2-dimethyl-1,3-benzodioxole was 37.8 g (87%). m.p. 87–89, ^{1}H NMR, δ: 1.67 (s, 6 H, C(2)Me_2); 6.98 (s, 2 H, Ar). FT-IR (KBr pellet): (cm^{-1}) = 2979 (=C–H), 1680, 1605, 1500 (C=C), 1250 (C–O).

4.3. Preparation of 5,6-dicyano-2,2-dimethyl-1,3-benzodioxole (**3**)

A mixture of 5,6-dibromo-2,2-dimethyl-1,3-benzodioxole (2.5 g, 8 mmol) and CuCN (3.63 g, 40 mmol) was refluxed in freshly distilled DMF (30 mL) for 3.5 h. The reaction mixture was cooled to 20 °C, and diluted with $CHCl_3$ (75 mL), whereby the precipitate formed. The precipitate was filtered off, and the filtrate was washed with water (5 × 100 mL) to remove DMF, dried over $CaCl_2$, and concentrated on a rotary evaporator. The residue was purified by column chromatography (silica gel, chloroform/n-hexane = 1/1), and yielded 0.56 g (35%) of **3**. m.p. 167–168 °C. ^{1}H NMR, δ: 1.67 (s, 6 H, C(2)Me_2); 7.03 (s, 2 H Ar). FT-IR (KBr pellet): (cm^{-1}) = 3064, 2994 (=C–H), 2229 (CN), 1596, 1502 (C=C), 1214 (C–O).

4.4. Preparation of zinc-2,3,9,10,16,17,23,24-tetra (isopropylidenedioxy) phthalocyanine (**4**)

A mixture of 4-tert-butyl-phthalonitrile (720 mg, 3.90 mmol), **3** (195.58 mg, 0.98 mmol), 1,8-diazabicyclo[5.4.0]undec-7-ene (DBU) (912 mg, 6.00 mmol), Zinc acetate ($Zn(AcO)_2$) (320 mg, 1.46 mmol) and pentanol (20 mL) was refluxed for 24 h [8]. After

cooling to room temperature, ether (20 mL) was added into the mixture, which was stirred for an additional 2 h. The precipitate was collected by filtration, and washed three times by ether. The crude product was purified by flash column chromatography (SiO_2, ethyl acetate/n-hexane = 1/3) to afford product **4** as a blue solid (160 mg, 20%). IR (KBr): ν = 3120, 2940, 1670, 1458, 1394, 1331, 1256, 1144, 1090, 1048, 922, 879 cm^{-1}; UV/Vis (EtOH): λ_{max} nm (Log ε) = 670 (0.325), 610 (0.050), 350 (0.115); MS (MALDI-TOF): *m/z*: 816.79–822.62 [M^+]; $C_{47}H_{44}N_8O_2Zn$ (816.29): calcd C 68.98, H 5.42, N 13.69; found C 68.67, H 6.09, N 11.52.

4.5. Preparation of tri-tert-butylcatecholphthalocyaninatozinc (*5*)

4 (160 mg, 0.195 mmol) was dissolved in concentrated H_2SO_4 (4 mL). The resulting solution was poured onto ice water (16 mL) immediately after the completed dissolution, whereby a precipitate formed. The precipitate was filtered off, washed with water, and dried under vacuum. The crude product was dissolved in dichloromethane and purified by re-precipitation in n-hexane. Yield 121.40 mg (80%). m.p. >300 °C. IR (KBr): ν = 3500–3100, 3120, 2940, 1670, 1458, 1394, 1331, 1256, 1144, 1090, 1048, 922, 879 cm^{-1}; UV/Vis (EtOH): λ_{max} nm (Log ε) = 680 (0.62), 610 (0.12), 350 (0.28); MS (MALDI-TOF): *m/z*: 776.47–781.48 [M^+]; $C_{47}H_{44}N_8O_2Zn$ (776.26): calcd C 67.90, H 5.18, N 14.49; found C 67.77, H 5.39, N 13.85.

4.6. Fabrication of DSSC

For the DSSC, a screen-printed double-layer film of interconnected TiO_2 particles was used as the mesoporous anode. First, an 8 μm thick film of 20-nm-sized TiO_2 particles (Solaronix) was printed on the fluorine-doped SnO_2 FTO (Pilkington, 8 Ω/sq) conducting glass electrode, which was pretreated with 40 mM $TiCl_4$ aqueous solution, referring to the earlier report of the Grätzel group [34]. Subsequently, a 4 μm thick second layer of 400-nm-sized light-scattering anatase particles (CCIC) was coated further on the first layer. The TiO_2 electrode was stained by immersing it into the dye solution containing 0.5 mM *ZnPc-Cat* in a mixture of anhydrous alcohol at room temperature for 18 h.

The sensitized titania electrode was assembled with a conducting Pt-counter electrode which was prepared by heating a FTO glass plate coated with two drops of 5 mM H_2PtCl_6 ethanol solution by means of a hot stream of air (380 °C) for 20 min. The electrolyte, of which composition and concentration was 0.6 M 3-propyl-1,2-dimethylimidazolium iodide, 0.05 M I_2, 0.1 M LiI, and 0.5 M TBP in a mixture of acetonitrile/valeronitrile (V/V = 1/1), was then introduced into the sandwiched cell with an architecture of FTO/20 nm-TiO_2/400 nm-TiO_2/Dye/Pt-FTO.

4.7. Photovoltaic characterization

The *ZnPc-Cat*-sensitized solar cells were measured employing a solar simulator equipped with a 400 W xenon lamp (Oriel), appropriate filters, and a digital source meter (Keithley model 2400) connected to a personal computer, which allows to determine photocurrents and photovoltages. The solar simulator was calibrated under global standard air mass (AM 1.5, 100 mW cm^{-2}) condition by employing KG5 filtered Si reference solar cell.

These measurements were carried out for dry film electrodes, and no corrections were made for optical effects due to the presence of the electrolyte. Photocurrent action spectra and photocurrent–photovoltage characteristics of the dye-sensitized TiO_2 electrodes were measured with sandwich-type cells. The working electrode of the dye-sensitized TiO_2 film on conducting glass was squeezed together with a platinized conducting glass using a spring and illuminated from the substrate side. The electrolyte, typically 0.5 M LiI/0.05 M I_2 in acetonitrile and valeronitrile, was attracted into the cavities of the dye-sensitized TiO_2 electrode by capillary forces. A 400 W xenon lamp with a monochromator was used as light source for the photocurrent action spectra measurements. The cell was operated in the short-circuit mode. The IPCE values were determined at 10 nm intervals between 300 and 900 nm. The IPCE was then calculated according to the following equation:

$$\mathrm{IPCE} = \frac{1240 i_{\mathrm{ph}}[\mu A]}{P[\mu W]\lambda[\mathrm{nm}]}$$

where i_{ph} and P are the photocurrent and power of the incident radiation per unit area and λ is the wavelength of the monochromatic light. No corrections were made for absorption and reflection in the substrate.

4.8. Incident photon-to-current conversion efficiency (IPCE)

The incident photon-to-current efficiency (IPCE) spectra were measured as a function of wavelength from 300 to 900 nm using a specially designed IPCE system (PV Measurements Inc.) for DSSCs. A similar data acquisition system was used to control the incident photon-to-current conversion efficiency (IPCE) measurement. Under full computer control, the light from a 400 W xenon lamp (ILC Technology) was focused through a Gemini-180 double monochromator (Jobin Yvon Ltd.) onto the photovoltaic cell under test. The monochromator was incremented through the visible spectrum to generate the IPCE (λ) as defined by IPCE (λ) 12,400 ($J_{sc}/\lambda\varphi$), where λ is the wavelength, J_{sc} is the short-circuit photocurrent density (mA cm^{-2}), and φ is the incident radiative flux (mW cm^{-2}). The photovoltaic performance was measured by using a metal mask with an aperture area of 0.159 cm^2. Solar cells covered with a 50 μm thick of polyester film (Preservation Equipment Ltd., UK) as a 400 nm UV cutoff filter were irradiated at open circuit under a Suntest CPS plus lamp (ATLAS GmbH, 100 mW cm^{-2}) in ambient air at 60 °C. The photovoltaic measurements were carried out at room temperature after allowing the cells to cool down and equilibrate during 2 h.

4.9. Electrochemical measurements

The electrochemical experiments were performed in a conventional three electrode cell with separate compartments for counter and reference electrodes at room temperature using a IVIUM compactstat. A 3-mm ITO glass acted as the working electrode, a saturated calomel electrode as the reference, and a platinum wire as the counter electrode, respectively. The ITO glass electrode was cleaned thoroughly in an ultrasonic water bath prior to each measurement. The electrolyte was 0.1 M tetrabutylammonium perchlorate in dry THF. The concentration of the dyes in the electrolyte was 0.5 mM.

Scans are initiated at 0 V versus SCE in positive direction at the rates of 50 mV/s. The solutions were purged with nitrogen and stirred for over 15 min prior to the measurements.

4.10. Other methods

UV/visible absorbance and emission spectra of the *ZnPc-Cat*-sensitized TiO_2 electrodes were recorded using a Perkin–Elmer Lambda 40 spectrophotometer and fluorescence spectrometer (Shimadzu RF-5000), respectively. Note that nanometer-sized TiO_2 was prepared by controlled hydrolysis of titanium(IV) tetraisopropoxide based on the earlier reports [35–37].

Nuclear magnetic resonance (NMR) spectra were obtained from a VARIAN UNITYINOVA 400 instrument. Infrared spectra were

taken using FT-IR Spectrophotometer (Nicolet). MALDI-TOF Mass analysis was carried out employing an instrument (Voyager DE-STR, Applied Biosystems) in a reflector mode with a matrix of 3,5-dimethoxy-4-hydroxy-trans-cinnamic acid (sinapinic acid) in all cases.

Acknowledgments

This work was supported by the Research Grant of University of Incheon in 2010. The authors appreciate the kind support of Prof. Lee, Wanin (Inha Univ.) for the IPCE measurement.

References

[1] O'Regan B, Grätzel M. A low-cost high-efficiency solar-cell based on dye sensitized colloidal TiO_2 films. Nature 1991;253:737–40.
[2] Nazeeruddin MK, Kay A, Rodicio I, Humphry-Baker R, Müller E, Liska P, et al. Conversion of light to electricity by cis-X2bis(2,2′-bipyridyl-4,4′ dicarboxylate) ruthenium(II) charge-transfer sensitizers ($X = Cl^-$, Br^-, I^-, CN^-, and SCN^-) on nanocrystalline titanium dioxide electrodes. J Am Chem Soc 1993;115:6382–90.
[3] Hagfeldt A, Grätzel M. Light-induced redox reactions in nanocrystalline systems. Chem Rev 1995;95:49–68.
[4] Nazeeruddin MK, Angelis FD, Fantacci S, Selloni A, Viscardi G, Liska P, et al. Combined experimental and DFT-TDDFT computational study of photo-electrochemical cell ruthenium sensitizers. J Am Chem Soc 2005;127:16835–47.
[5] Nazeeruddin MK, Zakeeruddin SM, Humphry-Baker R, Jirousek M, Liska P, Vlachopoulus N, et al. Acid-base equilibria of (2,2′-Bipyridyl-4,4′-dicarboxylic acid)ruthenium(II) complexes and the effect of protonation on charge-transfer sensitization of nanocrystalline titania. Inorg Chem 1999;38:6298–305.
[6] Tachibana Y, Haque SA, Mercer IP, Durrant JR, Klug DR. Electron injection and recombination in dye sensitized nanocrystalline titanium dioxide films: a comparison of ruthenium bipyridyl and porphyrin sensitizer dyes. J Phys Chem B 2000;104:1198–205.
[7] Koehorst RBM, Boschloo GK, Savenije TJ, Goossens A, Schaafsma TJ. Spectral sensitization of TiO_2 substrates by monolayers of porphyrin heterodimers. J Phys Chem B 2000;104:2371–7.
[8] He J, Benkö G, Korodi F, Polivka T, Lomoth R, Åkermark B, et al. Modified phthalocyanines for efficient near-IR sensitization of nanostructured TiO_2 electrode. J Am Chem Soc 2002;124:4922–32.
[9] He J, Hagfeldt A, Lindquist SE, Grennberg H, Korodi F, Sun L, et al. Phthalocyanine-sensitized nanostructured TiO_2 electrodes prepared by a novel anchoring method. Langmuir 2001;17:2743–7.
[10] Cid JJ, Yum JH, Jang SR, Nazeeruddin MK, Martínez-Ferrero E, Palomares E, et al. Molecular cosensitization for efficient panchromatic dye-sensitized solar cells. Angew Chem Int Ed 2007;46:8358–62.
[11] Montalti M, Wadhwa S, Kim WY, Kipp RA, Schmehl RH. Luminescent ruthenium(II) bipyridyl-phosphonic acid complexes: pH dependent photophysical behavior and quenching with divalent metal ions. Inorg Chem 2000;39:76–84.
[12] Moser J, Punchihewa S, Infelta PP, Grätzel M. Surface complexation of colloidal semiconductors strongly enhances interfacial electron-transfer rates. Langmuir 1991;7:3012–8.
[13] Rajh T, Chen LX, Lukas K, Liu T, Thurnauer MC, Tiede DM. Surface restructuring of nanoparticles: an efficient route for ligand-metal oxide crosstalk. J Phys Chem B 2002;106:10543–52.
[14] Tae EL, Lee SH, Lee JK, Yoo SS, Kang EJ, Yoon KB. A strategy to increase the efficiency of the dye-sensitized TiO_2 solar cells operated by photoexcitation of dye-to-TiO_2 charge-transfer bands. J Phys Chem B 2005;109:22513–22.
[15] Persson P, Bergström R, Lunell S. Quantum chemical study of photoinjection processes in dye-sensitized TiO_2 nanoparticles. J Phys Chem B 2000;104:10348–51.
[16] Frei H, Fitzmaurice DJ, Grätzel M. Surface chelation of semiconductors and interfacial electron transfer. Langmuir 1990;6:198–206.
[17] Tennakone K, Kumarasinghe AR, Kumara GRRA, Wijayantha KGU, Sirimanne PM. Nanoporous TiO_2 photoanode sensitized with the flower pigment cyaniding. J Photochem Photobiol A 1997;108:193–5.
[18] Rajh T, Nedeljkovic JM, Chen LX, Poluektov O, Thurnauer MC. Improving optical and charge separation properties of nanocrystalline TiO_2 by surface modification with vitamin C. J Phys Chem B 1999;103:3515–9.
[19] Ramakrishna G, Ghosh HN, Singh AK, Palit DK, Mittal JP. Dynamics of back-electron transfer processes of strongly coupled triphenyl methane dyes adsorbed on TiO_2 nanoparticle surface as studied by fast and ultrafast visible spectroscopy. J Phys Chem B 2001;105:12786–96.
[20] Dimitrijevic NM, Saponjic ZV, Bartels DM, Thurnauer MC, Tiede DM, Rajh T. Revealing the nature of trapping sites in nanocrystalline titanium dioxide by selective surface modification. J Phys Chem B 2003;107:7368–75.
[21] Wang Y, Hang K, Anderson NA, Lian T. Comparison of electron transfer dynamics in molecule-to-nanoparticle and intramolecular charge transfer complexes. J Phys Chem B 2003;107:9434–40.
[22] Huber R, Spörlein S, Moser JE, Grätzel M, Wachtveitl J. The role of surface states in the ultrafast photoinduced electron transfer from sensitizing dye molecules to semiconductor colloids. J Phys Chem B 2000;104:8995–9003.
[23] Ghosh HN, Asbury JB, Weng Y, Lian T. Interfacial electron transfer between $Fe(II)(CN)_6^{4-}$ and TiO_2 nanoparticles: direct electron injection and non-exponential recombination. J Phys Chem B 1998;102:10208–15.
[24] Cherepy NJ, Smestad GP, Grätzel M, Zhang JZ. Ultrafast electron injection: implications for a photoelectrochemical cell utilizing an anthocyanin dye-sensitized TiO_2 nanocrystalline electrode. J Phys Chem B 1997;10:9342–51.
[25] Mulliken RS. Molecular compounds and their spectra. II. J Am Chem Soc 1952; 74:811–24.
[26] Reddy PY, Giribabu L, Lyness C, Snaith HJ, Vijaykumar C, Chandrasekharam M, et al. Efficient sensitization of nanocrystalline TiO_2 films by a near-IR-absorbing unsymmetrical zinc phthalocyanine. Angew Chem Int Ed 2007; 46:373–6.
[27] Ivanov AV, Svinareva PA, Tomilova LG, Zefirov NS. Synthesis of 4,5-dihydroxyphthalonitrile. Russ Chem Bull Int Ed 2001;50:919–20.
[28] Brian WDA, Shubhashish D, Stephen RF, Peter D, Eugene P, Mark ET. Relationship between the ionization and oxidation potentials of molecular organic semiconductors. Org Electron 2005;6:11–20.
[29] Ramakrishna G, Jose DA, Kumar DK, Das A, Palit DK, Ghosh HN. Strongly coupled ruthenium–polypyridyl complexes for efficient electron injection in dye-sensitized semiconductor nanoparticles. J Phys Chem B 2005;109: 15445–53.
[30] Kar P, Verma S, Das A, Ghosh HN. Interfacial electron transfer dynamics involving a new bis-thiocyanate ruthenium(II)–polypyridyl complex, coupled strongly to nanocrystalline TiO_2, through a pendant catecholate functionality. J Phys Chem C 2009;113:7970–7.
[31] Ramakrishna G, Verma S, Jose DA, Kumar DK, Das A, Palit DK, et al. Interfacial electron transfer between the photoexcited porphyrin molecule and TiO_2 nanoparticles: effect of catecholate binding. J Phys Chem B 2006;110: 9012–21.
[32] Verma S, Kar P, Das A, Palit DK, Ghosh HN. Interfacial electron-transfer dynamics on TiO_2 and ZrO_2 nanoparticle surface sensitized by new catechol derivatives of Os(II)-polypyridyl complexes: monitoring by charge-transfer emission. J Phys Chem C 2008;112:2918–26.
[33] Kar P, Verma S, Sen A, Das A, Ganguly B, Ghosh HN. Sensitization of nanocrystalline TiO_2 anchored with pendant catechol functionality using a new tetracyanato ruthenium(II) polypyridyl complex. Inorg Chem 2010;49: 4167–74.
[34] Fan S, Li C, Yang G, Zhang L. Influence of $TiCl_4$ treatment on performance of dye- sensitized solar cell assembled with nano-TiO_2 coating deposited by vacuum cold spraying. Rare Metals 2006;25:163–8.
[35] Bahnemann D, Henglein A, Lilie J, Spanhel L. Flash photolysis observation of the absorption spectra of trapped positive holes and electrons in colloidal titanium dioxide. J Phys Chem 1984;88:709–11.
[36] Ghosh HN, Adhikari S. Trap state emission from TiO_2 nanoparticles in microemulsion solutions. Langmuir 2001;17:4129–30.
[37] Ramakrishna G, Ghosh HN. Optical and photochemical properties of sodium dodecylbenzenesulfonate (DBS)-capped TiO_2 nanoparticles dispersed in nonaqueous solvents. Langmuir 2003;19:505–8.